2012 IEEE International Conference on Robotics and Automation
RiverCentre, Saint Paul, Minnesota, USA
May 14-18, 2012

Simultaneous Optimization of Robot Trajectory and Nonlinear Springs to Minimize Actuator Torque

Nicolas Schmit and Masafumi Okada

***Abstract*— In this paper, we consider a robot with nonlinear springs located at each joints and acting in parallel with the actuators. We propose a method to simultaneously design the trajectory of the robot and the force/torque profiles of the springs for an optimal compensation of the gravity and inertial forces. First, we express the trajectory and force/torque profiles of the springs as a Hermite interpolation of a finite number of nodes, then we derive a closed-form solution of the optimal spring design as a function of the trajectory. As a consequence, the initial optimization problem is reduced to a trajectory optimization problem, solved with a numeric algorithm. We show an example of optimal design for a 3-Degree Of Freedom (DOF) serial manipulator. Finally, we show that the nonlinear springs calculated for this manipulator can be technically realized by a non-circular cable spool mechanism.**

I. INTRODUCTION

Robotic devices used for industrial processes are generally designed with very stiff links and joints to ensure an accurate positioning of the end-effector. In such robots, the actuators have to counteract not only the gravity forces but also the inertial forces of the links which magnitudes increase when the operating speed increases. If the actuators are not back-drivable (like when used with gears with high reduction ratios), the mechanical energy of the links can not be converted back to electric energy. Thus, decreasing the mechanical energy of the system requires to dissipate (*i.e.* lose) energy, and the amount of energy to dissipate increases with the operating speed.

So far, spring equilibrators have been developed to compensate for the gravity forces in manipulators [1–4] and the implementation of nonlinear springs in walking/running robots has proved to reduce the energy consumption [5, 6]. Compared to linear springs, nonlinear springs can realize complex load-displacement functions, so they can potentially result in a more energy-saving design. However, although optimal design methods have been proposed for gravity compensation and shock protection systems [7], few methods are available for the design of "energy buffers" based on nonlinear springs, except when the trajectory is known *a priori* [8]. In [9, 10], methods for a simultaneous design of trajectory and spring constants were proposed but they are restricted to linear stiffness.

This research is supported by the *Research on Macro/Micro Modeling of Human Behavior in the Swarm and its Control* under the Core Research for Evolutional Science and Technology (CREST) Program (research area: Advanced Integrated Sensing Technologies), Japan Science and Technology Agency (JST).

The authors are with the Department of Mechanical Sciences and Engineering, Tokyo Institute of Technology, 2-12-1 Ookayama, Meguro-ku, 152-8550 Tokyo, Japan schmit.n.aa@m.titech.ac.jp

In this paper, we consider a robot with nonlinear springs located at each joint and acting in parallel with the actuators. We propose a method to simultaneously design the trajectory of the robot and the torque profiles of the springs to minimize the actuator torques[1]. First, we discretize the trajectory and the nonlinear torque profiles of the springs with a finite number of parameters (thereafter referred as "trajectory parameters" and "spring parameters" respectively). Then, we show that the cost function of the optimization problem, defined as the integral of the actuator torques, is a quadratic function of the spring parameters. Thus, we can express the optimal spring parameters as a function of the trajectory parameters, and rewrite the optimization problem so that it depends only on the trajectory parameters. We use a Sequential Quadratic Programming (SQP) algorithm to optimize the trajectory. We show a example of optimal design for a 3-DOF serial manipulator. Finally, we show that the nonlinear springs calculated for this manipulator can be realized by a non-circular cable spool mechanism.

II. PROBLEM STATEMENT

A. Equations of motion

We consider a robot with n DOFs. Each joint is driven by an actuator and a nonlinear spring which act in parallel (the joint torque is the sum of the actuator torque and spring torque). Assuming that the mass-inertia parameters of the nonlinear springs are negligible compared with those of the system elements, the equations of motion of the robot can be written as

$$A(q)\ddot{q} + B(q, \dot{q}) = u(t) + w(q) \tag{1}$$

where t is the time, $q = (q_1(t), q_2(t), ..., q_n(t))^T$ is the column vector of joint variables, $u = (u_1(t), u_2(t), ..., u_n(t))^T$ is the column vector of actuator torques, $w = (w_1(q_1), w_2(q_2), ..., w_n(q_n))^T$ is the column vector of nonlinear spring torques, $A(q)$ is the mass matrix and $B(q, \dot{q})$ is a matrix which contains the Coriolis, centrifuge and gravity terms. Note that the torque of each nonlinear spring w_i depends only on the joint variable q_i of the joint where the spring is located. All w_i are continuously differentiable functions.

Different constraints are imposed on the trajectory, actuator torques and spring torques. These constraints have the form

[1] In this paper, we consider rotational springs and actuators. However, the design methodology is the same for prismatic springs and actuators.

$$\mathcal{G}\left(q(0),\dot{q}(0),q(T),\dot{q}(T)\right)=0 \tag{2}$$
$$\{q(t),\dot{q}(t)\}\in Q, t\in[0,T] \tag{3}$$
$$w(q)\in W, q\in[q_{min},q_{max}] \tag{4}$$
$$u(t)\in U, t\in[0,T] \tag{5}$$

where $\mathcal{G}$ are the boundary conditions, Q is a given domain of the phase space of the system under consideration, W and U are the set of permissible nonlinear spring torques and actuator torques respectively.

B. Cost function

We define the cost function of the optimization problem as the time integral of the actuator torques:

$$\mathcal{C}=\frac{1}{2}\int_0^T\|u(t)\|^2dt \tag{6}$$

where $t=0$ ant $t=T$ are the start and finish time of the motion.

We define $u_0(t)$ as the required actuator torque vector to achieve a given trajectory $q(t)$ when the joints are driven only by the actuators (no springs). $u_0(t)$ is calculated by inverse dynamics as

$$u_0(t)=A(q)\ddot{q}+B(q,\dot{q}) \tag{7}$$

When the joints are driven by both the actuators and nonlinear springs, the required actuator torque vector $u(t)$ to achieve a trajectory $q(t)$ is calculated as

$$u(t)=u_0(t)-w(q) \tag{8}$$

Substituting (8) in (6), we rewrite the cost function as

$$\begin{aligned}\mathcal{C}=&\frac{1}{2}\int_0^T\|u_0(t)\|^2dt-\int_0^T\langle u_0(t),w(q(t))\rangle\,dt\\&+\frac{1}{2}\int_0^T\|w(q(t))\|^2dt\end{aligned} \tag{9}$$

where $\langle\cdot,\cdot\rangle$ denotes the scalar product.

The optimization problem consists in finding the trajectory $q(t)$ and torque profiles of the nonlinear springs $w(q)$ which minimize $\mathcal{C}$ while satisfying the boundary conditions (2) and constraints (3)(4)(5).

III. PARAMETERIZATION OF THE TRAJECTORY AND SPRING TORQUE PROFILES

For each joint i, the range of the joint variable $[q_{i,min},q_{i,max}]$ is divided into N equal subintervals of length Δq_i. These intervals define $N+1$ nodes:

$$q_{i,j}=(j-1)\Delta q_i+q_{i,min},\quad j\in\{1..N+1\} \tag{10}$$

with $q_{i,N+1}=q_{i,max}$. A 3^{rd} order polynomial is used to represent the torque w_i of the i^{th} nonlinear spring on each subinterval. The value of w_i and its derivative at the nodes $q_{i,j}$ are used as design parameters. For each subinterval, the unique 3^{rd} order polynomial is defined that has values $(f_{i,j},f_{i,j+1})$ and derivatives $(s_{i,j},s_{i,j+1})$ at the end points of $[q_{i,j},q_{i,j+1})$. This definition allows the spring torque at any point $q_i=q_{i,j}+\rho_i\Delta q_i$ in $[q_{i,j},q_{i,j+1})$ to be written as

$$w_i(q_i)=\alpha_i\,f_{i,j+1}+\beta_i\,f_{i,j}+(\gamma_i\,s_{i,j+1}+\delta_i\,s_{i,j})\Delta q_i \tag{11}$$

where α_i, β_i, γ_i, δ_i are calculated as

$$\alpha_i=\rho_i^2(3-2\rho_i) \tag{12}$$
$$\beta_i=2\rho_i^3-3\rho_i^2+1 \tag{13}$$
$$\gamma_i=\rho_i^2(\rho_i-1) \tag{14}$$
$$\delta_i=\rho_i(\rho_i-1)^2 \tag{15}$$
$$\rho_i(q_i\in[q_{i,min},q_{i,max}))=\frac{q_i-q_{i,min}}{\Delta q_i}\mod 1 \tag{16}$$
$$\rho_i(q_{i,max})=1 \tag{17}$$

This scheme, called Hermite interpolation, automatically gives continuity of the torque and its derivative at the nodes. An example of torque profile is shown in Fig. 1.

From (11), the spring torque w_i at any point of $[q_{i,min},q_{i,max}]$ is calculated as

$$\begin{aligned}w_i(q_i)=&\sum_{j=1}^{N}[(\alpha_i\,f_{i,j+1}+\beta_i\,f_{i,j}\\&+(\gamma_i\,s_{i,j+1}+\delta_i\,s_{i,j})\Delta q_i)\,\chi_{i,j}(q_i)]\end{aligned} \tag{18}$$

$$\chi_{i,j}(q_i)=1\text{ if }q_i\in[q_{i,j},q_{i,j+1}) \tag{19}$$
$$\chi_{i,j}(q_i)=0\text{ if }q_i\notin[q_{i,j},q_{i,j+1}) \tag{20}$$
$$\chi_{i,N}(q_{i,max})=1 \tag{21}$$

where the functions $\chi_{i,j}$ are the indicator functions of the subintervals $[q_{i,j},q_{i,j+1})$. We gather all the design parameters $(f_{i,j},s_{i,j}\Delta q_i)$ in a vector y_i, and rewrite (18) as[2]

$$w_i(q_i)=\psi_i^T(q_i)y_i \tag{22}$$
$$\begin{aligned}y_i=&[f_{i,1},\ (s_{i,1}\Delta q_i),\ \ldots,\ f_{i,j},\ (s_{i,j}\Delta q_i),\ \ldots,\\&f_{i,N+1},\ (s_{i,N+1}\Delta q_i)]^T\end{aligned} \tag{23}$$
$$\begin{aligned}\psi_i(q_i)=&[\beta_i\chi_{i,1},\ \delta_i\chi_{i,1},\ \ldots,\ (\alpha_i\chi_{i,j-1}+\beta_i\chi_{i,j}),\\&(\gamma_i\chi_{i,j-1}+\delta_i\chi_{i,j}),\ \ldots,\ \alpha_i\chi_{i,N},\ \gamma_i\chi_{i,N}]^T\end{aligned} \tag{24}$$

[2]We use $s_{i,j}\Delta q_i$ instead of $s_{i,j}$ so that all elements of y_i have the same dimension.

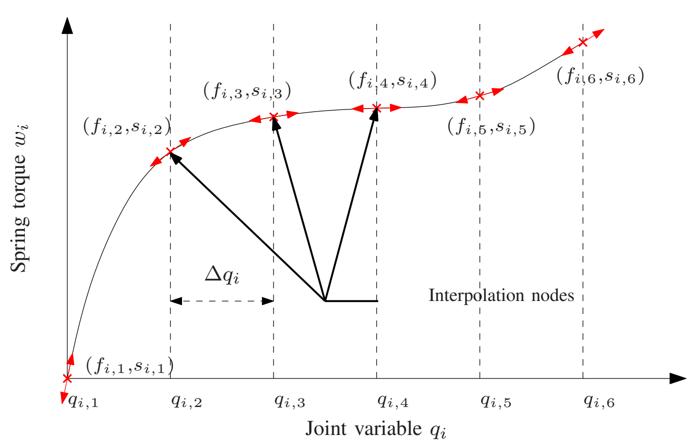

Fig. 1. Interpolation of a spring torque profile. The values of the torque $f_{i,j}$ and its derivative $s_{i,j}$ at each node are used as design parameters. On each subinterval, the torque is expressed by a third order polynomial uniquely defined by its values and derivatives at the endpoints of the subinterval.

Finally, the vector of all spring torques is expressed as

$$w(q) = \Psi^T(q)Y \tag{25}$$
$$Y = [{y_1}^T, ..., {y_n}^T]^T \tag{26}$$
$$\Psi(q) = \mathrm{blockdiag}\,(\psi_1(q_1), ..., \psi_n(q_n)) \tag{27}$$

where the operator blockdiag stands for "block diagonal matrix". $\Psi(q)$ is a matrix function of the joint variables, and Y is a vector which contains the interpolation data points of all torque profiles of the nonlinear springs. The elements of Y are thereafter referred as "spring parameters".

The trajectory is parameterized in a similar way, the only difference being that the interpolation nodes are the same for all DOFs (because the time variable is the same for all DOFs). The total time interval $[0, T]$ is divided into N_t equal subintervals of length Δt. These intervals define N_t+1 nodes:

$$t_k = (k-1)\Delta t, \;\; k \in \{1..N_t+1\}, \;\; \text{with } t_{N_t+1} = T \tag{28}$$

A 3^{rd} order polynomial is used to represent the joint variable q_i on each subinterval. The value of the position $x_{i,k}$ and velocity $v_{i,k}$ at the nodes t_k are used as design parameters. Using a similar methodology as for the parameterization of the torque profiles of the nonlinear springs, we express the i^{th} joint variable as

$$q_i(t) = \varphi_i^T(t) x_i \tag{29}$$
$$\begin{aligned} x_i = [&x_{i,1}, \;\; (v_{i,1}\Delta t), \;\; ..., \;\; x_{i,k}, \;\; (v_{i,k}\Delta t), \;\; ..., \\ &x_{i,N_t+1}, \;\; (v_{i,N_t+1}\Delta t)]^T \end{aligned} \tag{30}$$
$$\begin{aligned} \varphi_i(t) = [&\beta\tau_1, \;\; \delta\tau_1, \;\; ..., \;\; (\alpha\tau_{k-1} + \beta\tau_k), \\ &(\gamma\tau_{k-1} + \delta\tau_k), \;\; ..., \;\; \alpha\tau_{N_t}, \;\; \gamma\tau_{N_t}]^T \end{aligned} \tag{31}$$

where the functions τ_k are the indicator functions of the subintervals $[t_k, t_{k+1})$. Finally, the vector of all joint variables is expressed as

$$q(t) = \Phi^T(t)X \tag{32}$$
$$X = [{x_1}^T, ..., {x_n}^T]^T \tag{33}$$
$$\Phi(t) = \mathrm{blockdiag}\,(\varphi_1(t), ..., \varphi_n(t)) \tag{34}$$

$\Phi(t)$ is a time dependent matrix. X contains the interpolation data points of all DOFs of the trajectory. The elements of X are thereafter referred as "trajectory parameters".

Thereafter, the optimization problem consists in finding the trajectory parameters X and spring parameters Y which minimize $\mathcal{C}$ while satisfying (2)(3)(4)(5).

IV. OPTIMIZATION OF SPRING AND TRAJECTORY PARAMETERS

A. *Cost function at optimal spring design*

Substituting (25) in (9), we rewrite the cost function as

$$\begin{aligned} \mathcal{C}(X,Y) = &\frac{1}{2}\int_0^T \|u_0(t)\|^2 dt - \int_0^T Y^T \Psi(q(t)) u_0(t) dt \\ &+ \frac{1}{2}\int_0^T Y^T \Psi(q(t)) \Psi^T(q(t)) Y dt \end{aligned} \tag{35}$$

Since Y is not time-dependent, we can rewrite $\mathcal{C}$ as

$$\mathcal{C}(X,Y) = \mathcal{C}_0(X) - Z^T(X)Y + \frac{1}{2} Y^T K(X) Y \tag{36}$$
$$\mathcal{C}_0(X) = \frac{1}{2}\int_0^T \|u_0(t)\|^2 dt \tag{37}$$
$$Z(X) = \int_0^T \Psi(q(t)) u_0(t) dt \tag{38}$$
$$K(X) = \int_0^T \Psi(q(t)) \Psi^T(q(t)) dt \tag{39}$$

K is a symmetric matrix, Z is a vector, $\mathcal{C}_0$ is a scalar. K, Z and $\mathcal{C}_0$ are functions of the trajectory parameters X but independent from the spring parameters Y.

Formally, the optimal parameters (X^*, Y^*) are obtained by minimizing $\mathcal{C}$ with respect to X and Y simultaneously:

$$\left.\frac{\partial \mathcal{C}(X,Y)}{\partial X}\right|_{X=X^*} = 0 \tag{40}$$
$$\left.\frac{\partial \mathcal{C}(X,Y)}{\partial Y}\right|_{Y=Y^*} = 0 \tag{41}$$

However, since (36) is a quadratic function of Y, we can solve (41) and express the optimal spring parameters as a function of the trajectory parameters[3].

$$Y^*(X) = K^{-1}(X) Z(X) \tag{42}$$

Substituting (42) in (36), we define the *cost function at optimal spring design* $\mathcal{C}^*$ as

$$\mathcal{C}^*(X) = \mathcal{C}(X, Y^*(X)) = \mathcal{C}_0(X) - \frac{1}{2} Z^T(X) K^{-1}(X) Z(X) \tag{43}$$

Since the the optimization of the nonlinear springs is "embedded" in $\mathcal{C}^*$, this function depends only on the trajectory parameters X. The first term of $\mathcal{C}^*$ evaluates the trajectory when the robot is driven only by the actuators, and the second term evaluates the improvement due to the contribution of the nonlinear springs.

B. *Adjusting the nonlinearity of the springs*

Depending on the trajectory parameters, the optimal spring parameters can result in highly nonlinear torque profiles which could not be possible to realize by any mechanical device. Thus, in order to control the nonlinearity of the springs, we add to (36) a term which weights the second derivative of the nonlinear spring torques. The new cost function is

$$\begin{aligned} \mathcal{C}(X,Y) = &\mathcal{C}_0(X) - Z^T(X)Y + \frac{1}{2} Y^T K(X) Y \\ &+ \frac{1}{2}\sum_{i=1}^{n}\left[\frac{\lambda_i}{N\Delta q_i}\int_{q_{i,min}}^{q_{i,max}} \left(\frac{d^2 w_i(q_i)}{dq_i^2}\right)^2 dq_i\right] \end{aligned} \tag{44}$$

[3] K can become ill-conditioned if N is large (*i.e.* when trying to optimize spring torque profiles with many interpolation nodes). However, since we want to design springs which can be realized technically, we usually use a small N (smaller than 8) in order to obtain smooth torque profiles.

λ_i are weighting coefficients that the designer can modify to adjust the nonlinearity of the torque profiles. The higher the values of λ_i, the more linear the springs. If all λ_i are set to zero, (44) is equivalent to (36).

Substituting, (22) in (44), we rewrite the new term as

$$\frac{1}{2}\sum_{i=1}^{n}\left[\frac{\lambda_i}{N\Delta q_i} y_i^T \int_{q_{i,min}}^{q_{i,max}} \frac{d^2\psi_i}{dq_i^2}\frac{d^2\psi_i^T}{dq_i^2}\, dq_i\, y_i\right] \tag{45}$$

We decompose ψ_i as follows

$$\psi_i = \sum_{j=1}^{N} \widetilde{\psi}_{i,j}\,\chi_{i,j} \tag{46}$$

$$\widetilde{\psi}_{i,j} = [\underbrace{0..0}_{2(j-1)\text{zeros}}, \beta_i, \delta_i, \alpha_i, \gamma_i, \underbrace{0..0}_{2(N-j)\text{zeros}}]^T \tag{47}$$

where α_i, β_i, γ_i, δ_i, $\chi_{i,j}$ were defined in (12), (13), (14), (15), (19) respectively. Substituting (46) in (45), we obtain

$$\frac{1}{2}\sum_{i=1}^{n}\left[\frac{\lambda_i}{N(\Delta q_i)^4} y_i^T \sum_{j=1}^{N}\left(\int_0^1 \frac{d^2\widetilde{\psi}_{i,j}}{d\rho_i^2}\frac{d^2\widetilde{\psi}_{i,j}^T}{d\rho_i^2}\, d\rho_i\right) y_i\right] \tag{48}$$

where ρ_i was defined in (16). Since α_i, β_i, γ_i, δ_i are 3^{rd} order polynomials of ρ_i, the integral term in (48) is equal to

$$\left[\frac{d\widetilde{\psi}_{i,j}}{d\rho_i}\frac{d^2\widetilde{\psi}_{i,j}^T}{d\rho_i^2}\right]_{\rho_i=0}^{\rho_i=1} - \left[\widetilde{\psi}_{i,j}\frac{d^3\widetilde{\psi}_{i,j}^T}{d\rho_i^3}\right]_{\rho_i=0}^{\rho_i=1} \tag{49}$$

Calculating (49) from the equations of α_i, β_i, γ_i, δ_i, (48) is equal to

$$\frac{1}{2}\sum_{i=1}^{n}\left[\frac{\lambda_i}{N(\Delta q_i)^4} y_i^T\, Q\, y_i\right] \tag{50}$$

where the matrix Q is calculated as

$$Q = \begin{bmatrix} Q_0 & Q_2 & & & \\ Q_2^T & Q_3 & \ddots & & \\ & \ddots & \ddots & \ddots & \\ & & \ddots & Q_3 & Q_2 \\ & & & Q_2^T & Q_1 \end{bmatrix} \tag{51}$$

$$Q_0 = \begin{bmatrix} 12 & 6 \\ 6 & 4 \end{bmatrix} \tag{52}$$

$$Q_1 = \begin{bmatrix} 12 & -6 \\ -6 & 4 \end{bmatrix} \tag{53}$$

$$Q_2 = \begin{bmatrix} -12 & 6 \\ -6 & 2 \end{bmatrix} \tag{54}$$

$$Q_3 = \begin{bmatrix} 24 & 0 \\ 0 & 8 \end{bmatrix} \tag{55}$$

Finally, (44) is equivalent to

$$\mathcal{C}(X,Y) = \mathcal{C}_0(X) - Z^T(X)Y + \frac{1}{2}\,Y^T K(X) Y + \frac{1}{2}\,Y^T G Y \tag{56}$$

where the matrix G is defined as

$$G = \text{blockdiag}\left(\frac{\lambda_1}{N(\Delta q_1)^4}\,Q, ..., \frac{\lambda_n}{N(\Delta q_n)^4}\,Q\right) \tag{57}$$

We see that we can control the nonlinearity of the spring torque profiles by adding to the cost function a term $\frac{1}{2}Y^T GY$, where the matrix G is symmetric. From (56), we derive the cost function at optimal spring design:

$$\mathcal{C}^*(X) = \mathcal{C}_0(X) - \frac{1}{2}\,Z^T(X)(K(X)+G)^{-1}Z(X) \tag{58}$$

If all weighting coefficients λ_i are set to zero, (58) is equivalent to (43). Note that since the matrix Q is constant, it can be calculated before the optimization process in order to reduce the total calculation cost.

C. *Optimization of trajectory parameters*

In Section IV-A we defined a cost function $\mathcal{C}^*$ which depends only on the trajectory parameters. However, since this function is highly nonlinear, it is not possible to derive a closed form expression of the optimal trajectory parameters except for a few simple cases. Thus, we use an SQP algorithm to find an approximate solution of the optimal trajectory. Details on SQP methods can be found in [11]. When using an SQP algorithm, it is required to provide an explicit expression of the cost function $\mathcal{C}^*$ and its gradient $\Delta_X\mathcal{C}^*$. Due to space limitations, we do not detail the calculation of $\Delta_X\mathcal{C}^*$ in this paper.

V. EXAMPLE OF OPTIMAL DESIGN

We consider the 3-DOF serial manipulator shown in Fig. 2. ℓ_i is the length of link i, h_i is the distance from the origin of the coordinate frame attached to link i to the link's center of mass, θ_i is the angular displacement of coordinate frame i with respect to coordinate frame $(i-1)$ (coordinate frame 0 is the reference frame), and g is the acceleration of gravity.

As design constraints, we impose the end effector to stop at prescribed positions during chosen time intervals. These constraints are summarized in Table I. From time 0s to 1s, the end effector must stop to coordinates (30, 10, 20), from time 5s to 6s, the end effector must stop to coordinates (60, 80, 40), etc. Note that we imposed a same constraint at $t = 0$s and $t = 20$s in order to synthesize a periodic motion. The vector of parameters λ_i defined in Section IV-B was set to $[0.2, 0.00007, 0.00007]^T$.

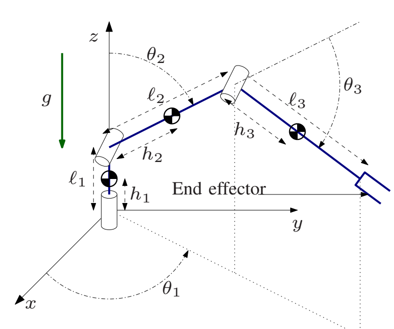

Fig. 2. 3-DOF serial manipulator

TABLE I

CONSTRAINTS ON THE TRAJECTORY

	t (s)	x (cm)	y (cm)	z (cm)
p_1	[0, 1]	30	10	20
p_2	[5, 6]	60	80	40
p_3	[10, 11]	-50	-40	70
p_4	[15, 16]	-50	100	120
p_5	20	30	10	20

The initial and optimal trajectories are shown in Fig. 3. The labels p_1 to p_5 indicate the constrained parts of the trajectory. The initial and optimal paths are shown in Fig. 4. The green line shows the path of the end effector. The manipulator (in blue) is drawn at time $t = 8$s. The label p_5 is not displayed because if would appear exactly above the label p_1.

In the left column of Fig. 5, we show the restoring torques of the nonlinear springs. The dashed line shows the location of the interpolation nodes of the torque profiles. An increasing restoring torque corresponds to positive stiffness while a decreasing restoring torque corresponds to negative stiffness. In the right column of Fig. 5, we show the torque applied to each joint by its nonlinear spring (blue solid line), its actuator (red solid line), and the total torque (black x-mark line). We can see on Fig. 5(d) and Fig. 5(f) that a significant part of the total torque is provided by the nonlinear springs, thus reducing the average actuator torque. In Table II, we show the value of the cost function C^* for a robot driven by actuators only and for a robot driven by actuators and optimal nonlinear springs. From this table, we understand that the design with the best performances is obtained by a simultaneous optimization of the trajectory and the nonlinear spring torque profiles.

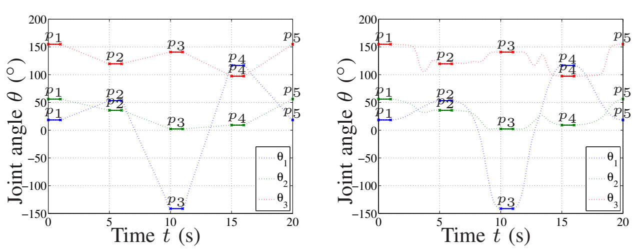

(a) Initial design (b) Optimal design

Fig. 3. Trajectory of manipulator (joint variables)

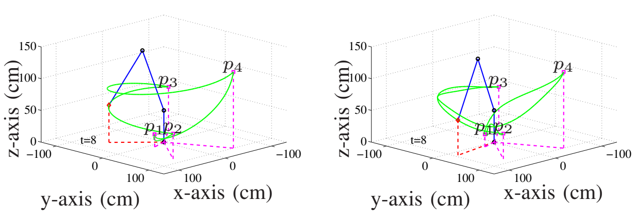

(a) Initial design (b) Optimal design

Fig. 4. Path of end effector

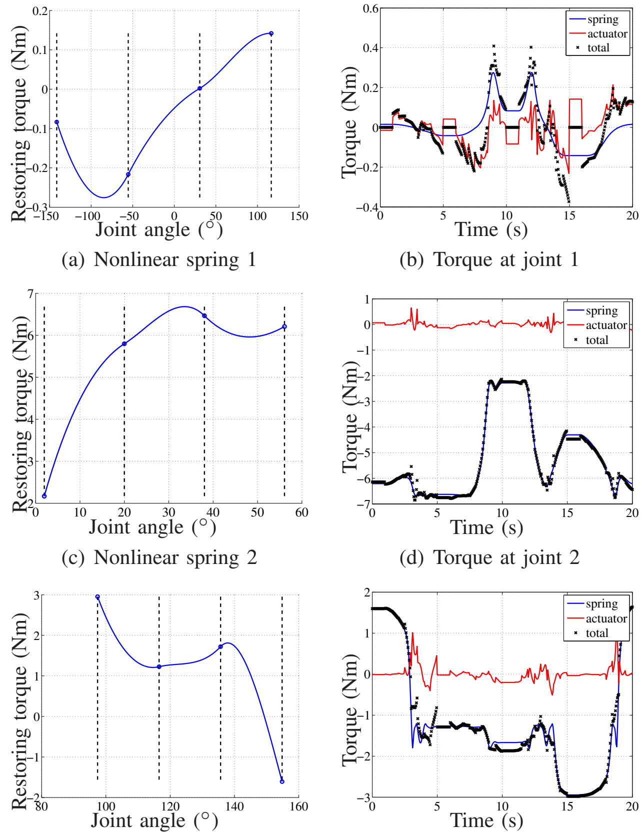

(a) Nonlinear spring 1 (b) Torque at joint 1

(c) Nonlinear spring 2 (d) Torque at joint 2

(e) Nonlinear spring 3 (f) Torque at joint 3

Fig. 5. Spring torque profiles and joint torques

TABLE II

COST FUNCTION C^*

	No spring	With optimal nonlinear springs
Initial trajectory	322	6.28
Optimal trajectory	124	0.681

VI. TECHNICAL REALIZATION OF THE NONLINEAR SPRINGS

The spring synthesized in Section V are highly nonlinear and exhibit negative stiffness on a part of their displacement range. Since these springs do not correspond to any off-the-shelf spring, we propose to realize them with the mechanism shown in Fig. 6. This mechanism consists in a linear spring connected to a cable wound around a non-circular spool which shape is calculated so that the mechanism behaves as a nonlinear rotational spring with the prescribed torque profile [12].

Since the cable-spool mechanism can only handle positive torques, the nonlinear springs 1 and 3 are realized by the antagonistic action of two cable-spool mechanisms. The first ones realizes the torque profiles of Fig. 7(a), Fig. 8(a), Fig. 9(a), calculated by shifting the torque profiles of Section V vertically so that the torque is strictly positive. A reduction ratio is introduced between the joint and the spool to adjust the rotation range of the spool. The second mechanism realizes a constant spring, so that the antagonistic action of the two mechanisms achieves the torque profiles of Section

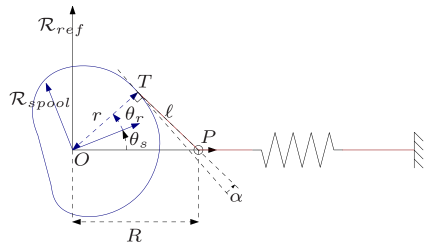

Fig. 6. Transmission mechanism with a non-circular cable spool

V. The shape of the spool synthesizing the shifted torque profiles are shown in Fig. 7(b), Fig. 8(b) and Fig. 9(b). See [12] for the realization of the constant springs.

VII. CONCLUSIONS

In this paper, we proposed a method to simultaneously design the trajectory of a robot and the torque profiles of nonlinear springs acting in parallel with the actuators in order to minimize the average actuator torque. We first expressed the trajectory and the torque profiles of the spring using a third order Hermite interpolation, and used the interpolation points as the design parameters. We showed that the cost function is a quadratic function of the spring parameters, and expressed the optimal spring parameters as a function of the trajectory parameters. By doing so, we defined a *cost function at optimal spring design* which depends only on the trajectory parameters. We used a SQP algorithm to find an approximate solution of the optimal trajectory. We showed that the nonlinearity of the springs can be adjusted (from linear to highly nonlinear) by adding to the cost function a weighting matrix G. As an example, we proposed the optimal design of a 3-DOF serial manipulator. Several constraints were set on the position of the manipulator for given time domains, while the algorithm was let free to optimize the unconstrained parts of the trajectory. The results showed that a significant part of the overall joint torque was provided by the nonlinear springs, resulting in a significant decrease in the average actuator torque required to drive the robot. We showed that the nonlinear springs calculated in this paper were technically realizable using a non-circular cable spool mechanism.

Since the nonlinear springs buffer the mechanical energy, we expect the actuation of the manipulator designed in Section V to be significantly less energy consuming than a system without springs. The analysis of energy consumption will be addressed in future work.

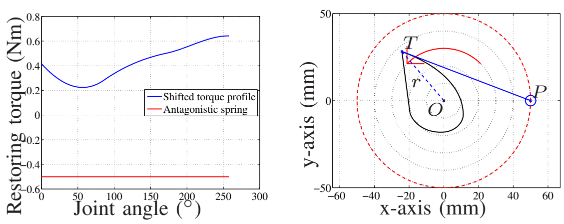

(a) Shifted torque profile (b) Spool

Fig. 7. Realization of spring 1 with a non-circular spool mechanism

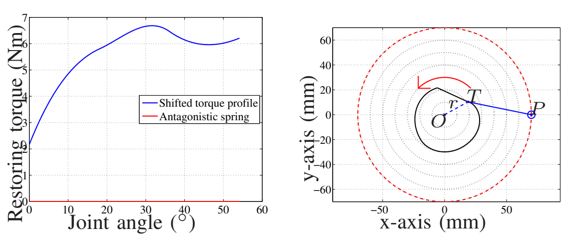

(a) Shifted torque profile (b) Spool

Fig. 8. Realization of spring 2 with a non-circular spool mechanism

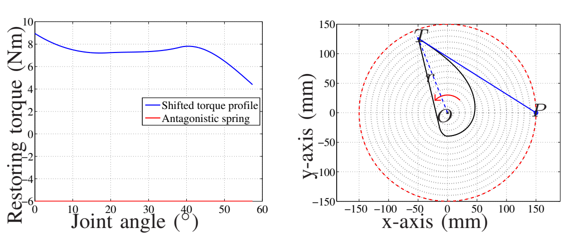

(a) Shifted torque profile (b) Spool

Fig. 9. Realization of spring 3 with a non-circular spool mechanism

REFERENCES

[1] G. J. Walsh, D. A. Streit, and B. J. Gilmore. "Spatial spring equilibrator theory". In: *Mechanism and Machine Theory* 26.2 (1991), pp. 155–170.

[2] Doo Y. Jo, Edward J. Haug, and Ronald R. Beck. *Optimization of force balancing mechanisms*. Tech. rep. A101421. Iowa City, IA 52242, USA: College of Engineering, The University of Iowa, Mar. 1982.

[3] D. A. Streit and B. J. Gilmore. "Perfect Spring Equilibrators for Rotatable Bodies". In: *Journal of mechanisms, transmissions, and automation in design* 111.4 (1989), pp. 451–458.

[4] N. Ulrich and V. Kumar. "Passive mechanical gravity compensation for robot manipulators". In: *Proc. IEEE International Conference on Robotics and Automation*. Vol. 2. Sacramento, CA, USA, Apr. 1991, pp. 1536 –1541.

[5] J. Yamaguchi, D. Nishino, and A. Takanishi. "Realization of dynamic biped walking varying joint stiffness using antagonistic driven joints". In: *Proc. IEEE International Conference on Robotics and Automation*. Vol. 3. Leuven, Belgium, May 1998, pp. 2022–2029.

[6] R. McN. Alexander. "Three uses for springs in legged locomotion". In: *International Journal of Robotics Research* 9.2 (Apr. 1990), pp. 53–61.

[7] E. Suhir. "Shock protection with a nonlinear spring". In: *IEEE Transactions on Components, Packaging, and Manufacturing Technology* 18.2 (June 1995), pp. 430–437.

[8] V. E. Berbyuk and A. E. Bostrom. "Optimization Problems of Controlled Multibody Systems Having Spring-Damper Actuators". In: *International Applied Mechanics* 37 (7 2001), pp. 935–940.

[9] T. Schauss, M. Scheint, M. Sobotka, W. Seiberl, and M. Buss. "Effects of compliant ankles on bipedal locomotion". In: *IEEE International Conference on Robotics and Automation*. Kobe, Japan, May 2009, pp. 2761 –2766.

[10] Katja D. Mombaur, Richard W. Longman, Hans Georg Bock, and Johannes P. Schloder. "Open-loop stable running". In: *Robotica* 23.01 (2005), pp. 21–33.

[11] Alex Barclay, Philip E. Gill, and J. Ben Rosen. "SQP methods and their application to numerical optimal control". In: *Variational calculus, optimal control, and applications*. Ed. by Werner H. Schmidt Leonhard Bittner Rolf Kltzler. Vol. 124. International Series of Numerical Mathematics. Birkhuser, 1998, pp. 207–222.

[12] Nicolas Schmit and Masafumi Okada. "Synthesis of a Non-Circular Cable Spool to Realize a Nonlinear Rotational Spring". In: *Proc. IEEE International Conference on Intelligent Robots and Systems*. San Francisco, CA, USA, Sept. 2011.